Density Functional Theory and Molecular Dynamic Studies About Effects of Functionalization and Surface Modification of Graphene on Adsorption of Phosgene

Karimi, Pouya**+; Poorsargol, Mahdiye; Sanchooli, Mahmood
Department of Chemistry, Faculty of Science, University of Zabol, Zabol, I.R. IRAN

ABSTRACT: *Adsorption of phosgene on the surface of a graphene sheet was studied. The surface of this material was modified through a metamaterial approach using heteroatoms (N and B), the addition of hydrogen atoms, and functionalized with four CHO groups at edges to survey the role of defects, Hydrogen Bonding (HB), and Intramolecular Hydrogen Bonding (IHB) interactions on adsorption. Generally, there is repulsion between the π-electron cloud of the graphene sheet and electrons of electronegative atoms on pollutants. However, the addition of hydrogen atoms to the surfaces of this material leads to the formation of attractive HB interactions with pollutants such as phosgene. Also, heteroatoms have helpful effects on the adsorption process. Therefore, the adsorption of phosgene on a modified graphene sheet is better than that of pristine graphene. Results of Molecular Dynamic (MD) simulations expose that van der Waals (vdW) and HB interactions have major contributions to the adsorption of phosgene on modified graphene.*

KEYWORDS: *Metamaterial; Pollutants; Intramolecular hydrogen bonding; Charge transfer; Binding energy.*

INTRODUCTION

Functionalization of graphene sheets is a way to improve the capability of this nano-material for the adsorption of pollutants. Covalent functionalizations of graphene sheets lead to the enhancement of thermal and electronic conductivity, solubility, and selectiveness of the related composites [1, 2]. Thus, functionalized graphene sheets have outstanding applications in electronics [3, 4], energy [5], biomedicine [6, 7], catalysis [8,9], and environmental sciences [10, 11]. Graphene-based nano-materials have a large specific surface area and porous composition. These features make them good adsorbents for pollutants [12], supercapacitors [13], and ions [14-16]. It seems that functional groups at the edges of the graphene sheets facilitate interplays with pollutants. Accordingly, investigation of such forces can help to improve the selectiveness and performance of adsorbents [17].

Graphene has hydrophobic properties, but function-alized graphene sheets show hydrophilic characteristics [18]. Functionalization of graphene with hydroxyl and carboxylic acid groups has been reported [19]. Moreover,

* *To whom correspondence should be addressed.*
+ E-mail: pkarimi@uoz.ac.ir
1021-9986/2023/8/2427-2437 11/$/6.01

other functional groups such as amine [20], amide [21], thio [22], and nitro [23] can attach to the edges of graphene. Mesoporous materials such as SBA-15 have been used for hydroisomerization and hydrocracking of n-heptane [24] and are also efficient carriers in drug delivery [25]. Recently, functionalized MCM-41 was introduced for the delivery of curcumin as an anti-inflammatory therapy [26]. Indeed, MCM-48 and Amine-Grafted MCM-48 have been utilized for the adsorption of Cd (II) and Pb (II) in both cases affinity for adsorption of cadmium was more considerable than that for lead. [27]. Moreover, some authors studied the reduction of the Chemical Oxygen Demand (COD) for wastewater contaminated by phenolic compounds by three adsorption methods [28]. They reported a maximum removal rate of the COD equal to 94 %.

Density Functional Theory (DFT) calculations have been formerly performed to obtain quantitative data about the nature of interactions of some pollutants and drugs with various graphene sheets [29-32]. Also, the removal of organic dyes using a graphene sheet has been studied [33]. Pesticides and chlorinated molecules can form hydrogen bond interactions with graphene and functionalized graphene sheets. Adsorption of such molecules by graphene-based materials has been previously studied [34, 35]. Functional groups may change the distribution of charges on the graphene sheet and adjust its tendency for interactions with various species [36].

Phosgene is a very poisonous gas and is used for the production of precursors of polyurethanes and polycarbonate plastics [37]. Moreover, chloroform can convert into phosgene upon ultraviolet radiation in the presence of oxygen [38]. Additionally, carbon tetrachloride turns into phosgene in air at high temperatures [39]. Therefore, it is necessary to study materials that have a good affinity for the adsorption of this gas. In the present study, we utilized a (3,3) graphene sheet with 15 Å length and replaced two C atoms at the central ring with N or B atoms to probe the role of the defect in the graphene structure on adsorption of phosgene using quantum mechanical studies and Molecular Dynamic (MD) simulations. Indeed, a hydrogen atom was added to one of the N atoms at the central ring of the later graphene sheet to survey the effect of Hydrogen Bonding (HB) interaction on the adsorption of phosgene. Furthermore, all graphene sheets were functionalized with four CHO groups. As can be seen in Fig. 1, the CHO groups construct four Intramolecular Hydrogen Bond (IHB) interactions at the edges of these graphene sheets. The IHB interaction is an important force in which proton donor and proton acceptor parts exist in one molecule.

Besides, in resonance-assisted hydrogen bond (RAHB) interaction two ends of a π-conjugated system are connected by IHB interaction [40, 41]. These interactions have been formerly studied in various molecular systems [42-47]. The two practical applications of the RAHB systems are molecular memories and molecular switches [48, 49]. Afterward, interactions of the phosgene with central rings of the mentioned graphene sheets were monitored using quantum mechanical calculations and MD simulations. Various factors include structural parameters, energy data, electron charge densities, electronic properties, charge transfer (CT), thermochemistry data, Lennard-Jones (L-J) and electrostatic energies, and formation of hydrogen bonding were investigated to find capability of the mentioned graphene sheets for adsorption of phosgene. The main purpose of this work is modification of structure of the graphene sheet to propose suitable modified graphenes for better adsorption of the pollutants such as phosgene.

Computational methods

Geometries were optimized at the M06-2X/6-31G** level of theory using the Gaussian09 program package [50]. Vibrational frequencies were calculated on optimized structures. The topological properties of electron charge densities were calculated by Atoms In Molecules (AIM) method using AIM2000 program [51].

The GROMOS 54 A7 force field was selected to represent all bonded and non-bonded interactions [52]. Automated Topology Builder (ATB) was used to generate topology and conformation of phosgene and graphene sheets [53]. Long-range electrostatic interactions were calculated using the Particle Mesh Ewald (PME) method [54]. The cut-off distance for the van der Waals interactions was taken as 1.2 nm.

Before starting MD simulation, energy minimization was carried out using the steepest descent method [55]. Subsequently, the system was put through NVT ensemble at 298 K for 100 ps and then continued employing NPT ensemble for 100 ps at 298 K and 1 bar using Nose–Hoover thermostat and Parrinello–Rahman barostat [56, 57]. The MD simulation was performed via NPT ensemble for 5 ns with the integration time step of 1 fs. Equations of motion were integrated using the Verlet algorithm [58].

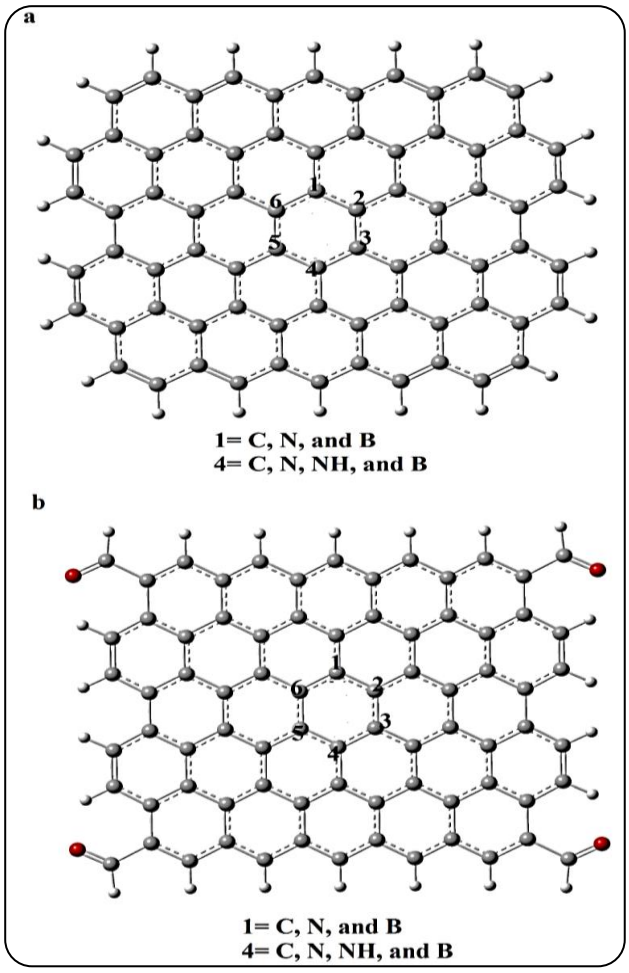

Fig. 1: Presentation of the structure of graphene (a) and functionalized graphenes (b) together with numbers of the most important atoms

These simulations were carried out using the GROMACS package version 4.6 [55]. The visualization of structures was performed using PyMOL software [59].

RESULTS AND DISCUSSION

A (3,3) graphene sheet with 15 Å length was selected to survey the role of structural modification and functionalization on the adsorption of phosgene using quantum mechanical studies and MD simulations (Fig. 1). First, the two C atoms at the central ring of this graphene sheet were replaced with two N or two B atoms to explore the role of heteroatom on adsorption. Then, a hydrogen atom was added to one of the N atoms at the central ring of the graphene sheet to examine the role of HB interaction on the adsorption process. Finally, all graphene sheets were functionalized with four CHO groups to seek the role of IHB interactions on the adsorption of phosgene. Alteration of the structure of the graphene sheet using a metamaterial approach is a plan to discover modified graphene sheets with good capacities for the adsorption of pollutants such as phosgene.

Energy data

There are various pollutants with different structures and computational approaches help to estimate the strength of intermolecular interactions between these molecules and graphene sheets. The graphene sheet and functionalized graphene sheets utilized in the present study are shown in Fig. 1. The intermolecular interactions between the phosgene and these graphene sheets were considered to get better insight into the adsorption of phosgene on such materials. The seven binary complexes are graphene-phosgene, graphene 2N-phosgene, graphene 2B-phosgene, graphene 2NH-phosgene, graphene 4CHO-phosgene, graphene 2N 4CHO-phosgene, and graphene 2B 4CHO-phosgene that are denoted as G_1, G_2, G_3, G_4, G_5, G_6, and G_7, respectively.

The interaction energy (ΔE) for each binary complex AB is defined as:

$$\Delta E = E_{AB} - (E_A + E_B) \quad (1)$$

In this study, the complexes AB are G_1, G_2, G_3, G_4, G_5, G_6, and G_7. The monomers A and B refer to the graphene sheet (or functionalized graphene sheets) and phosgene, respectively. Binding energy (BE) is considered as $-\Delta E$ and is a benchmark for the strength of the interaction in each binary complex. All estimated binding energies are gathered in Table 1. As can be seen, the replacement of two C atoms at the central ring of the graphene sheet with two N or two B atoms leads to an increase in BE values of complexes G_2 and G_3 in comparison to complex G_1. Moreover, the addition of a hydrogen atom to one of N atoms at the central ring of the graphene sheet brings about to suitable interaction between phosgene and the proposed graphene sheet with the largest BE value in complex G_4. In fact, a HB interaction is formed in complex G_4. On the other hand, functionalization of the graphene sheet and modified graphene sheets using four CHO groups at edges is accompanied by a decrease of BE values of the complexes G_5, G_6, and G_7 in comparison to the corresponding complexes without IHB interactions (G_1, G_2, and G_3, respectively). Accordingly, functionalization of the graphene sheets in such a way that aids the formation of the HB interaction

Table 1: Surface area (Å^2) and electronic properties of the graphene and functionalized graphenes (eV), and binding energies of their complexes with phosgene (kcal/mol)

Molecule	Surface area	[a]E_{HOMO}	[a]E_{LUMO}	[a]EG	[a]μ	[b]BE
G_1	894.94	-4.931	-2.709	2.222	-3.82	4.50
G_2	901.42	-4.967	-1.817	3.150	-3.39	4.94
G_3	912.77	-5.833	-2.591	3.243	-4.21	5.26
G_4	917.80	-4.122	-2.111	2.011	-3.12	7.48
G_5	990.18	-5.377	-3.130	2.246	-4.25	4.32
G_6	990.54	-5.388	-2.350	3.038	-3.87	4.74
G_7	1006.35	-5.477	-2.592	2.885	-4.03	5.00

a: for monomers; b: for complexes

between these beds and phosgene is a proposal technique for better adsorption of such pollutants on them.

The BE values versus distance between the graphene and functionalized graphene sheets with phosgene (R) is depicted in Fig. 2.

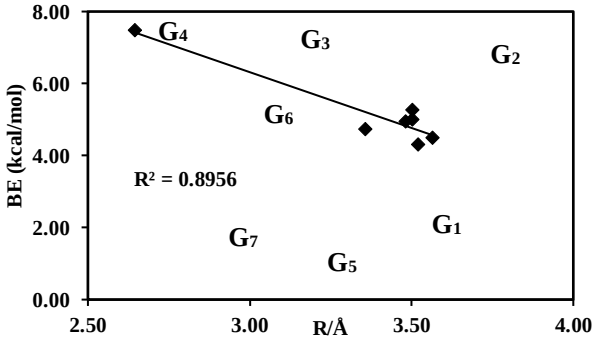

Fig. 2: The binding energies of the complexes as a function of distances between graphene and functionalized graphenes with phosgene

As can be seen, the increase of BE values is relatively followed by a decrease of R. Energies of Highest Occupied Molecular Orbital (HOMO) and Lowest Unoccupied Molecular Orbital (LUMO), and Energy Gap (EG) values of the graphene sheet and functionalized graphene sheets are listed in Table 1.

Results revealed that there is no direct relationship between these data and BE values. Indeed, chemical potential (μ) values were calculated as:

$$\mu = -(I + A)/2 \quad (2)$$

I and A is ionization potential and electron affinity, respectively. However, there isn't a meaningful connection between the chemical potentials of these materials and BE values. It seems that other electronic factors effect on magnitudes of the BE values. Also, dipole moment (D) values of all graphene sheets were calculated to find the role of charge separation on the BE values. There is a linear relationship between BE values of the complexes and dipole moments of the graphene sheets with linear regression coefficient R=0.96. Results show that modified graphene 2B and graphene 2NH sheets related to complexes G_3 and G_4 have more dipole moments in comparison to other ones. As said, G_3 and G_4 have larger BE values than other complexes. Thus, making more charge separation in the graphene sheet using surface modification may help to better the interaction of it with phosgene and similar pollutants. This result suggests that polarizing graphene sheets using heteroatoms and the addition of hydrogen atoms may improve the surfaces of these materials for the adsorption of pollutants that encompass halogen atoms. Moreover, the surface area of the graphene sheets was estimated and listed in Table 1. Surface area is a very important factor in increasing the adsorption rate [60]. The data show that modification of the graphene sheet is accompanied by an increase in surface area. Furthermore, the increase in surface area is relatively followed by an increase in the BE values. It should be noted that the graphenes are insoluble in aqueous media. However, the dispersion may somewhat occur under ultra-sonication conditions or vigorous stirring. Also, phosgene is insoluble in water. Therefore, the main aim of surface modification is to increase of surface area of the graphenes that can facilitate the adsorption of pollutants such as phosgene on these materials.

Analysis of Atomic charges

The atomic charges of all structures were calculated to better understand the role of Charge Transfer (CT) on the adsorption of phosgene on the graphene sheet and functionalized graphene sheets. The presented data in Table 2 show the sum of atomic charges on phosgene in the complexes is negative. Thus, the direction of overall CT is from the graphene sheets to the phosgene.

As can be seen in Fig. 3, the decrease in negative CT is relatively followed by an increase in BE values of the complexes.

Also, the sum of atomic charges at the central rings of the graphene sheet and functionalized graphene sheets and

Table 2: The most important atomic charges in the graphene and functionalized graphenes, and corresponding complexes with phosgene (e)

Molecule	[a]q	[b]q	[c]q
G_1	0.052	0.038	-0.015
G_2	-0.591	-0.595	-0.009
G_3	-0.214	-0.229	-0.011
G_4	-0.703	-0.697	-0.001
G_5	0.062	0.047	-0.014
G_6	-0.589	-0.593	-0.008
G_7	-0.201	-0.217	-0.011

a: Charge of the central ring in monomer; b: Charge of the central ring in the complex; c: Charge of phosgene in complex

Table 3: Properties of electron charge densities of graphene sheets and their complexes with phosgene (au)

Molecule	[a]ρ_{RCP} ×10^2	[b]ρ_{RCP} ×10^2	[b]ρ_{CCP} ×10^4
G_1	2.030	2.059	5.408
G_2	2.010	2.014	5.246
G_3	1.952	1.943	5.026
G_4	2.017	2.016	5.817
G_5	2.032	2.037	5.524
G_6	2.009	2.014	5.377
G_7	1.956	1.949	5.046

a: for monomers; b: for complexes

all complexes were calculated. Central rings of the modified graphene sheets encompass more negative charges than the graphene sheet. On the other hand, functionalization of the graphene sheet and modified graphene sheets with four CHO groups causes a decrease of negative atomic charges at central rings. It seems that the sum of atomic charges at the mentioned rings have an effect on the BE values. Results point out that the sum of atomic charges at the central ring of the graphene sheet is less than the functionalized graphene sheet with four CHO groups. Also, the mentioned atomic charges in the modified graphene sheets are more negative than the corresponding graphene sheets with four CHO groups. Accordingly, BE value of the complex **G_1** is larger than **G_5**. Also, there is a similar relationship between BE values of the complexes **G_2** and **G_6**, as well as **G_3** and **G_7**. Moreover, the largest BE value is related to complex **G_4** and results show that the sum of atomic charges at the central ring of its matching modified graphene sheet is more negative than other ones. As a result, modification and functionalization of the graphene sheets help to control the distribution of atomic charges on their rings. It seems that this factor

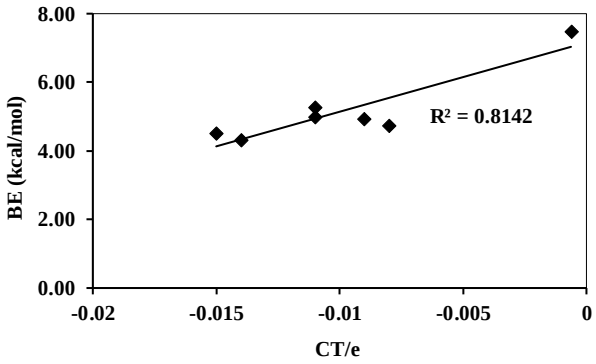

Fig. 3: Relationship between binding energies of the complexes and magnitudes of the charge transfer to phosgene

influences on the quality and quantity of adsorption of pollutants on surfaces of these materials.

AIM study

AIM analyses were performed to determine the relationship between topological properties of electron charge densities and BE values. Topological parameters of the graphene sheets and corresponding complexes are gathered in Table 3.

The electron charge density at ring critical point (ρ_{RCP}) and cage critical point (ρ_{CCP}) were evaluated. Functionalization of the graphene sheet and modified graphene sheets with four CHO groups leads to alteration of the ρ_{RCP} values. As said, the mentioned functionalization has an effect on the sum of atomic charges at the central rings of these materials. The decrease of negative atomic charges at the central rings of these materials is parallel with the increase of the ρ_{RCP} values. It seems that this charge distribution is a factor that makes BE values of the complexes G_5, G_6, and G_7 smaller in comparison to the matching complexes without IHB interactions (G_1, G_2, and G_3, respectively). Also, the ρ_{CCP} values for the complexes G_5, G_6, and G_7 are larger than those for the analogous complexes G_1, G_2, and G_3, respectively. On the other hand, complex G_4 has the largest ρ_{CCP} value among other complexes. Really, the formation of the HB interaction in complex G_4 is accompanied by an increase of electron charge density at Cage Critical Point (CCP) and plays an important role on stability of this complex. Thus, functionalization of the graphene sheets using IHB interactions and formation of the HB interaction between these materials and pollutants such as phosgene influence on magnitudes of the ρ_{CCP} values and stability of the resultant complexes.

Table 4: Thermochemistry data related to the interaction of graphene sheets with phosgene

Molecule	[a]ΔH	[b]ΔG	[c]ΔS × 10^2
G_1	-648495.36	-648497.68	0. 78
G_2	-648531.94	-648540.69	2.94
G_3	-648532.00	-648540.65	2.90
G_4	-648535.11	-648542.08	2.34
G_5	-648532.04	-648537.95	1.98
G_6	-648532.38	-648538.73	2.13
G_7	-648531.79	-648540.22	2.83

a and b in kcal/mol, and c in kcal mol/K

Thermochemistry data

The enthalpy of formation (ΔH), Gibbs free energy of formation (ΔG), and entropy of formation (ΔS) for all binary complexes were calculated and gathered in Table 4.

Results specify that modification and functionalization of the graphene sheet alter ΔG values for adsorptions of phosgene on resulting materials. Actually, ΔG values for all complexes are more negative than that for complex G_1. Thus, surface modification of the graphene sheet leads to better adsorption of the phosgene thermodynamically on the modified graphene sheets. Also, the decrease of ΔG is relatively in harmony with an increase in the BE values of all complexes (with the exception of complex G_1). It seems that the distribution of charge on graphene sheets influences on thermochemistry of the adsorption process. The Molecular Electrostatic Potential (MEP) maps of the graphene sheets and corresponding binary complexes have depicted in supplementary material (Fig. S1). As can be observed, graphene provides a rich electron region (red) that is favorable for accepting hydrogen atoms of molecules with acidic hydrogen. However, phosgene has chlorine atoms and there is a repulsive interaction between the mentioned red region of graphene and electrons of chlorine atoms. On the other hand, functionalization and surface modification of graphenes leads to the decrease of electron enrichment on the central rings of these materials. Consequently, phosgene can better adsorb on functionalized and modified graphenes than pristine graphene.

Infra-Red (IR) spectra of the proposed materials (graphene sheet, modified graphene sheets, and functionalized graphene sheets) and all complexes were theoretically computed and represented in supplementary material (Fig. S2). Comparison of the IR spectrum of each material with its binary complex shows that there is a pick for adsorption of phosgene. This pick refers to the stretching vibrational frequency of the C=O bond. There is repulsion between electrons of chlorine atoms and π-electron clouds of the mentioned surfaces. The intensity of this pick is lower in complex G_4 than those in other complexes. As said, phosgene can close to the surface of the modified graphene sheet via attractive HB interaction in complex G_4. Also, BE value of this complex is larger than other complexes. This result accentuates the role of attractive interactions between surfaces of graphene-like materials and pollutants such as phosgene on the quality and quantity of the adsorption process. Moreover, the repulsive interaction between chlorine atoms of the phosgene and the π-electron cloud of the functionalized graphene sheets is diminished. Therefore, these graphene sheets can also be utilized for the adsorption of other pollutants such as SO_2, NO_2, and CO_2 that have electronegative oxygen atoms.

Molecular dynamic simulations

Following quantum mechanical calculations, MD simulations were performed to examine dynamic adsorption behavior of the phosgene on the surfaces of the graphene sheets. To this end, graphene 2N, graphene 2B, and graphene 2NH sheets were selected because of their superior performance in phosgene adsorption. In all the simulated systems, graphene sheet was positioned and held in the center of the simulation box by applying a constant force of 1000 kJ/mol nm^2. Subsequently, a phosgene molecule was positioned approximately 20 Å above the central ring of the graphene sheet. The simulation snapshots of the initial and final configurations of complex G_4 are shown in Fig. 4.

Accordingly, the phosgene molecule is adsorbed on the surface of graphene 2NH after the MD simulation. Due to the large number of snapshots, only those related to G_4 adsorption system are displayed. The simulation snapshots of G_2 and G_3 adsorption systems also show the adsorption of phosgene molecules on surfaces of the graphene 2N and graphne 2B, respectively. The distance between the center of mass of the phosgene and each modified graphene sheet (R) was measured during the simulation time. As seen in Fig. 5, the adsorption distances between phosgene and the modified graphene sheets are declined and stabilized after 1 ns. The mean distance between the center of mass of

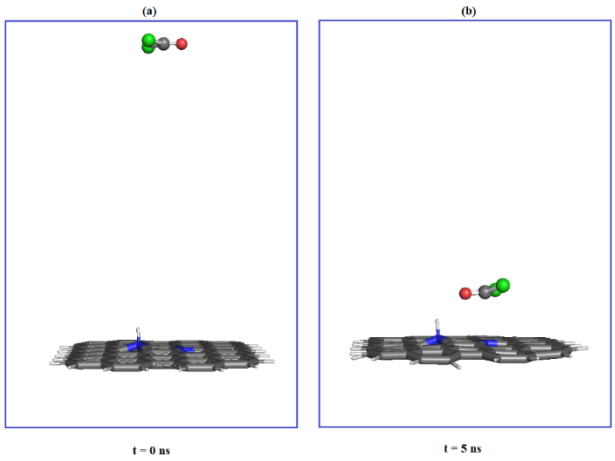

Fig. 4: Representative initial simulation snapshot of phosgene configuration on graphene 2NH surface before equilibrium (a) and after equilibrium (b)

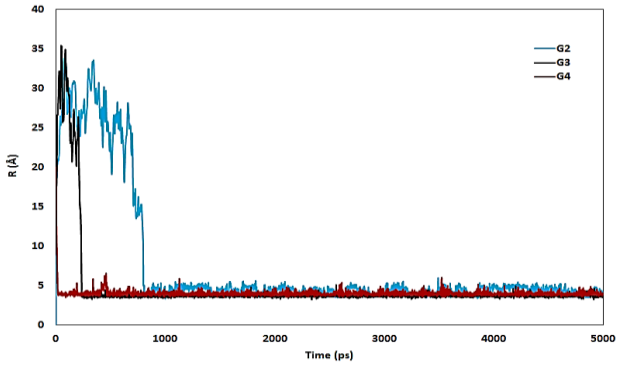

Fig. 5: The adsorption distance between the center of mass of the phosgene and modified graphene sheets (R) as a function of simulation time

phosgene and the modified graphene sheet in complexes G_2, G_3, and G_4 was 7.6, 4.7, and 3.9 Å, respectively. Evidently, in complex G_4, the phosgene molecule lays on the shortest distance from corresponding modified graphene sheet. This trend is similar to the results of quantum mechanical calculations and indicates the better and faster adsorption of phosgene on graphene 2NH surface.

The mean electrostatic and Lennard-Jonse (L-J) energies between phosgene and the graphene sheets were calculated during the simulation to study the interactions between phosgene and the mentioned graphene sheets. The order of absolute values of the electrostatic energies in the selected complexes is G_2 (0.27) < G_3 (1.18) < G_4 (6.33). Also, the order of absolute values of the L-J energies is G_2 (26.97) < G_3 (29.53) < G_4 (30.67). As can be seen, the highest electrostatic and L-J energies refer to complex G_4. This finding indicates that the strength of electrostatic and van der Waals (vdW) interactions between phosgene and graphene 2NH sheet in complex G_4 are greater than those for complexes G_2 and G_3. Therefore, modification of graphene sheet via the addition of hydrogen atoms and heteroatoms increases the desirable interactions of phosgene with it. Indeed, the lowest electrostatic and L-J energies belong to complex G_2. This declining trend of energy values is similar to the decreasing trend of BE values obtained from quantum mechanical calculations for these complexes. Furthermore, the L-J energies are greater than the electrostatic ones, suggesting that the vdW forces have the largest contribution in the interaction between phosgene and the mentioned graphene sheets. As a result, the non-bonded vdW interactions are a key factor in the stability of these three complexes. Moreover, HB interaction was explored during the simulation process to specify the formation of the HB between phosgene and graphene 2NH surface in complex G_4. The number of HBs formed between phosgene and graphene 2NH surface as a function of the simulation time are illustrated in Fig. 6. As can be seen, an intermolecular HB was formed between phosgene and graphene 2NH surface during the simulation trajectory that has a significant effect on phosgene adsorption. Therefore, the HB interactions between phosgene and graphene 2NH surface greatly contribute to the stability of complex G_4.

CONCLUSIONS

The adsorption of phosgene on a graphene sheet and some functionalized graphene sheets were estimated using DFT studies and MD simulations. Adsorption of phosgene on the graphene sheet and modified graphene sheets is better in comparison to materials that functionalized with IHB interactions. The results show that surface modification of the graphene sheet via heteroatoms (N, NH, and B) has a constructive effect on the adsorption process. The addition of hydrogen atoms to the modified graphene sheets may help to the formation of attractive HB interactions between surfaces of these materials and pollutants such as phosgene. Graphenes with larger dipole moments can form stable complexes with phosgene. There is a negative charge transfer from the graphenes to phosgene. Adsorption of phosgene on modified graphene

sheets is enhanced in comparison to pristine graphene. Results of MD simulations reveal that vdW and HB interactions can be considered among the most significant binding forces between phosgene and modified graphenes.

Acknowledgments

We thank the University of Zabol for all its supports. The Grant number of this work is IR-UOZ-GR-9923.

Received : Nov. 26, 2022 ; Accepted : Jan. 16, 2023

REFERENCES

[1] Xiang Z., Dai Q., Chen J.-F., Dai L., Edge Functionalization of Graphene and Two-Dimensional Covalent Organic Polymers for Energy Conversion and Storage, *Adv. Mater.*, **28**: 6253-6261 (2016).

[2] Bueno R.A., Martínez J.I., Luccas R.F., del Árbol N.R., Munuera C., Palacio I., Palomares F.J., Lauwaet K., Thakur S., Baranowski J.M., Strupinski W., López M.F., Mompean F., García-Hernández M., Martín-Gago J.A., Highly Selective Covalent Organic Functionalization of Epitaxial Graphene, *Nat. Commun.*, **8**: 15306 (2017).

[3] Scidà A., Haque S., Treossi E., Robinson A., Smerzi S., Ravesi S., Borini S., Palermo V., Application of Graphene-Based Flexible Antennas in Consumer Electronic Devices, *Mater. Today.*, **21**: 223-230 (2018).

[4] Zhao J., Liu C., Ma J.A., A Light-Driven Modulation of Electric Conductance through the Adsorption of Azobenzene onto Silicon-Doped- and Pyridine-Like N3-Vacancy Graphene, *Nanoscale*, **9**: 19017-19025 (2017).

[5] Li X., Zhi L., Graphene Hybridization for Energy Storage Applications, *Chem. Soc. Rev.*, **47**: 3189-3216 (2018).

[6] Zeng Y., Yang Z., Li H., Hao Y., Liu C., Zhu L., Liu J., Lu B., Li R., Multifunctional Nanographene Oxide for Targeted Gene-Mediated Thermochemotherapy of Drug-resistant Tumour, *Sci. Rep.*, **7**: 1-10 (2017).

[7] Kenry L.W.C., Loh K.P., Lim C.T., When Stem Cells Meet Graphene: Opportunities and Challenges in Regenerative Medicine, *Biomaterials*, **155**: 236-250 (2018).

[8] Ye R., Dong J., Wang L., Mendoza-Cruz R., Li Y., An P.F., Yacamán M.J., Yakobson B.I., Chen D., Tour J.M., Manganese Deception on Graphene and Implications in Catalysis, *Carbon.*, **132**: 623-631 (2018).

[9] Rana S., Jonnalagadda S.B., Synthesis and Characterization of Amine Functionalized Graphene Oxide and Scope as Catalyst for Knoevenagel Condensation Reaction, *Catal. Commun.*, **92**: 31-34 (2017).

[10] Ren X., Li J., Chen C., Gao Y., Chen D., Sue M., Alsaedi A., Hayat T., Graphene Analogues in the Aquatic Environment and Porous Media: Dispersion, Aggregation, Deposition and Transformation, *Environ. Sci.: Nano.*, **5**: 1298-1340 (2018).

[11] Othman N.H., Alias N.H., Shahruddin M.Z., Abu Bakar N.F., Him N.R.N., Lau W.J., Adsorption Kinetics of Methylene Blue Dyes onto Magnetic Graphene Oxide, *J. Environ. Chem. Eng.*, **6**: 2803-2811 (2018).

[12] Zhang X., Gao B., Creamer A.E., Cao C., Li Y., Adsorption of VOCs onto Engineered Carbon Materials: A Review, *J. Hazard. Mater.*, **338**: 102-123 (2017).

[13] Targholi E., Mousavi Khoshdel S.M., Rahmanifar M., Impact of Structural Defects in the Functionalized Graphene with –COOH on the Efficiency of Graphene-Based Supercapacitors, *Iran. J. Chem. Chem. Eng. (IJCCE)*, **35**: 33-42 (2016).

[14] Karimi P., Effects of Structure and Partially Localization of the π Electron Clouds of Single-Walled Carbon Nanotubes on the Cation-π Interactions, *Iran. J. Chem. Chem. Eng. (IJCCE)*, **35(3)**: 35-43 (2016).

[15] Karimi P., Sanchooli M., Investigation of Ability of Graphene Based Nanostructures as Sodium Ion Batteries, *Iran. J. Chem. Chem. Eng. (IJCCE)*, **38**: 23-30 (2019).

[16] Alipour F. M., Mirzaagha Babazadeh; Esmail Vessally; Akram Hosseinian; Parvaneh Delir Kheirollahi Nezhad, A Computational Study on the Some Small Graphene-Like Nanostructures as the Anodes in Na−Ion Batteries, *Iran. J. Chem. Chem. Eng. (IJCCE)*, **40**: 691-703 (2021).

[17] Kyhl L., Bisson R., Balog R., Groves M.N., Kolsbjerg E.L., Cassidy A.M., Jørgensen J.H., Halkjær S., Miwa J.A., Čabo A.G., Angot T., Hofmann P., Arman M.A., Urpelainen S., Lacovig P., Bignardi L., Bluhm H., Knudsen J., Hammer B., Hornekaer L., Exciting H2 Molecules for Graphene Functionalization, *ACS Nano*, **12**: 513-520 (2018).

[18] Petosa A.R., Jaisi D.P., Quevedo I.R., Elimelech M., Tufenkji N., Aggregation and Deposition of Engineered Nanomaterials in Aquatic Environments: Role of Physicochemical Interactions, *Environ. Sci. Technol*., **44**: 6532-6549 (2010).

[19] Wang J., Yu S., Zhao Y., Wang X., Wen T., Yang T., Ai Y., Chen Y., Hayat T., Alsaedi A., Wang X., Experimental and Theoretical Studies of ZnO and MgO for the Rapid Coagulation of Graphene Oxide from Aqueous Solutions, *Sep. Purif. Technol*., **184**: 88-96 (2017d).

[20] Wanjeri V.W.O., Sheppard C.J., Prinsloo A.R.E., Ngila J.C., Ndungu P.G., Isotherm and Kinetic Investigations on the Adsorption of Organophosphorus Pesticides on Graphene Oxide Based Silica Coated Magnetic Nanoparticles Functionalized with 2-Phenylethylamine, *J. Environ. Chem. Eng*., **6**: 1333-1346 (2018).

[21] Ahmed M.S., Kim Y.-B., Amide-Functionalized Graphene with 1,4-Diaminobutane as Efficient metal-Free and Porous Electrocatalyst for Oxygen Reduction, *Carbon.*, **111**: 577-586 (2017).

[22] Mahmoodi N.M., Ghezelbash M., Shabanian M., Aryanasab F., Saeb M.R., Efficient Removal of Cationic Dyes from Colored Wastewaters by Dithiocarbamate-Functionalized Graphene Oxide Nanosheets: From Synthesis to Detailed Kinetics Studies, *J. Taiwan Inst. Chem. Eng.*, **81**: 239-246 (2017).

[23] Begum H., Ahmed M.S., Cho S., Jeon S., Simultaneous Reduction and Nitrogen Functionalization of Graphene Oxide Using Lemon for Metal-Free Oxygen Reduction Reaction, *J. Power Sources*., **372**: 116-124 (2017).

[24] Ali N.S., Alismaeel Z.T., Majdi H.Sh., Salih H.G., Abdulrahman M.A., Cata Saady N.M., Albayati T.M., Modification of SBA-15 Mesoporous Silica as an Active Heterogeneous Catalyst for the Hydroisomerization and Hydrocracking of n-Heptane, *Helyion*, **8**: e09737 (2022).

[25] Atiyah N.A., Albayati T.M., Atiya M.A., Interaction Behavior of Curcumin Encapsulated onto Functionalized SBA-15 as an Efficient Carrier and Release in Drug Delivery, *J. Mol. Struc.*, **1260**: 132879 (2022).

[26] Atiyah N.A., Albayati T.M., Atiya M.A., Functionalization of Mesoporous MCM-41 for the Delivery of Curcumin as an Anti-Inflammatory Therapy, *Adv. Powder. Technol*., **33**: 103417 (2022).

[27] Vatandoust H., Younesi H., Mehraban Z., Heidari A., Khakpour H., Comparative Adsorption of Cd (II) and Pb (II) by MCM-48 and Amine-Grafted MCM-48 in Single and Binary Component Systems, *Water Conserv. Sci. Eng.*, **6**: 67-78 (2021).

[28] Kadhum Sh.T., Alkindi Gh.Y., Albayati T.M., Determination of Chemical Oxygen Demand for Phenolic Compounds from Oil Refinery Wastewater Implementing Different Method, *Desalination Water Treat.*, **231**: 44-53 (2021).

[29] Li J., Wu Q., Wang X., Chai Z., Shi W., Hou J., Hayat T., Alsaedie A., Wang X., Heteroaggregation Behavior of Graphene Oxide on Zr-Based Metalorganic Frameworks in Aqueous Solutions: A Combined Experimental and Theoretical Study, *J. Mater. Chem. A*, **5**: 20398-20406 (2017).

[30] Zou Y., Wang X., Ai Y., Liu Y., Ji Y., Wang H., Hayat T., Alsaedi A., Hu W., Wang X., β-Cyclodextrin Modified Graphitic Carbon Nitride for the Removal of Pollutants from Aqueous Solution: Experimental and Theoretical Calculation Study, *J. Mater. Chem. A*, **4**: 14170-14179 (2016b).

[31] Vessally E., Musavi M., Poor Heravi M.R., A Density Functional Theory Study of Adsorption Ethionamide on the Surface of the Pristine, Si and Ga and Al-Doped Graphene, *Iran. J. Chem. Chem. Eng (IJCCE).*, **40(6)**: 1720-1736 (2021).

[32] Vessally E., Farajzadeh P., Najafi E., Possible Sensing Ability of Boron Nitride Nanosheet and Its Al– and Si–Doped Derivatives for Methimazole Drug by Computational Study, *Iran. J. Chem. Chem. Eng*., **40(4)**: 1001-1011 (2021).

[33] Naseri, A., Barati R., Rasoulzadeh F., Bahram M., Studies on Adsorption of Some Organic Dyes from Aqueous Solution onto Graphene Nanosheets, *Iran. J. Chem. Chem. Eng. (IJCCE)*, **34(2)**: 51-60 (2015).

[34] Lazarevic-Pasti T., Anicijevic V., Baljozovic M., Vasic Anicijevic D., Gutic S., V. Vasic V., Skorodumova N.V., Pasti I.A., The Impact of Structure of Graphene Based Materials on Removal of Organophosphorus Pesticides from Water, *Environ. Sci.: Nano*., **5**: 1482-1494 (2018).

[35] Chinthakindi S., Purohit A., Singh V., Tak V., Goud D.R., Dubey D.K., Pardasani D., Iron Oxide Functionalized Graphene Nano-Composite for Dispersive Solid Phase Extraction of Chemical Warfare Agents from Aqueous Samples, *J. Chromatogr. A*, **1394**: 9-17 (2015).

[36] Cai N., Larese-Casanova P., Application of Positively-Charged Ethylenediamine-Functionalized Graphene for the Sorption of Anionic Organic Contaminants from Water, *J. Environ. Chem. Eng.*, **4**: 2941-2951 (2016).

[37] Nakata M., Kohata K., Fukuyama T., Kuchitsu K., Molecular Structure of Phosgene as Studied by Gas Electron Diffraction and Microwave Spectroscopy. The r_z Structure and Isotope Effect, *J. Mol. Spect.*, **83**: 105-117 (1980).

[38] Pohl L.R., Bhooshan B., Whittaker N.F., Krishna G., Phosgene: A Metabolite of Chloroform, *Biochem. Biophys*., **79**: 684-691 (1977).

[39] Singh H.B., Phosgene in the Ambient Air, *Nature*, **264**: 428-429 (1976).

[40] Gilli G., Bellucci F., Ferretti V., Bertolasi V., Evidence for Resonance-Assisted Hydrogen Bonding from Crystal-Structure Correlations on the Enol Form of the β-Diketone Fragment, *J. Am. Chem. Soc*., **111**: 1023-1028 (1989).

[41] Bertolasi V., Gilli P., Ferretti V., Gilli G., Evidence for Resonance-Assisted Hydrogen Bonding. 2. Intercorrelation between Crystal Structure and Spectroscopic Parameters in Eight Intra-Molecularly Hydrogen Bonded 1,3-Diaryl-1,3-propanedione Enols, *J. Am. Chem. Soc*., **113**: 4917-4925 (1991).

[42] Grosch A.A., Van der Lubbe S.C.C., Guerra C.F., Nature of Intramolecular Resonance Assisted Hydrogen Bonding in Malonaldehyde and its Saturated Analogue, *J. Phys. Chem. A*, **122**: 1813-1820 (2018).

[43] Karimi P., Sanchooli M., Shojaa-Hormozzahi F., Estimation of Resonance Assisted Hydrogen Bond (RAHB) Energies Using Properties of Ring Critical Points in Some Dihydrogen-Bonded Complexes, *J. Mol. Strcut.*, **1242**: 130710 (2021).

[44] Rusinska-Roszak D., Intramolecular Hydrogen Bond Energy via O-H…O-C the Molecular Tailoring Approach to RAHB Structures, *J. Phys. Chem. A*, **119**: 3674-3687 (2015).

[45] Gurbanov A.V., Kuznetsov M.L., Demukhamedova S.D., Alieva I.N., Godjaev N.M., Zubkov F.I., Mahmudov K.T., Pombeiro A.J.L., Role of Substituents on Resonance Assisted Hydrogen Bonding vs. Intermolecular Hydrogen Bonding, *Cryst. Eng. Comm*., **22**: 628-633 (2020).

[46] Karimi P., Sanchooli M., Investigation of Resonance Assisted Hydrogen Bond (RAHB) in Some Pyridine-Based Complexes: Intramolecular and Intermolecular Interactions, *J. Mol. Strcut.*, **1204**: 127546-50 (2020).

[47] Karimi P., Sanchooli M., Tuning the Resonance-Assisted Hydrogen Bond (RAHB) of Malonaldehyde Using π-Conjugated Substituents and Presentation of its Energy Decomposition, *J. Mol. Graph. Model*., **112**: 108142 (2022).

[48] Douhal A., Sastre R., Room-Temperature Triple Proton Transfer of 7-Hydroxyquinoline and Stabilization of its Ground-State Keto Tautomer in a Polymeric Matrix, *Chem. Phys. Lett.*, **219**: 91-94 (1994).

[49] Sytnik A., Del Valle J.C., Steady-State and Time-Resolved Study of the Proton-Transfer Fluorescence of 4-Hydroxy-5-azaphenanthrene in Model Solvents and in Complexes with Human Serum Albumin, *J. Phys. Chem*., **99**: 13028-13032 (1995).

[50] Frisch M.J., Trucks G.W., Schlegel H.B., Scuseria G.E., Robb M.A., Cheeseman J.R., Scalmani G., Barone V., Mennucci B., Petersson G.A., Nakatsuji H., Caricato M., Li X., Hratchian H.P., Izmaylov A.F., Bloino J., Zheng G., Sonnenberg J.L., Hada M., Ehara M., Toyota K., Fukuda R., Hasegawa J., Ishida M., Nakajima T., Honda Y., Kitao O., Nakai H., Vreven T., J.A. Montgomery, Peralta Jr., J.E., Ogliaro F., Bearpark M., Heyd J.J., Brothers E., Kudin K.N., Staroverov V.N., Kobayashi R., Normand J., Raghavachari K., Rendell A., Burant J.C., Iyengar S.S., Tomasi J., Cossi M., Rega N., Millam J.M., Klene M., Knox J.E., Cross J.B., Bakken V., Adamo C., Jaramillo J., Gomperts R., Stratmann R.E., Yazyev O., Austin A.J., Cammi R., Pomelli C., Ochterski J.W., Martin R.L., Morokuma K., Zakrzewski V.G., Voth G.A., Salvador P., Dannenberg J.J., Dapprich S., Daniels A.D., Farkas O., Foresman J.B., Ortiz J.V., Cioslowski J., Fox D.J., Gaussian 09, Revision A.02, Gaussian, Inc., Wallingford CT (2009).

[51] Bader R. F. W., "Atoms in Molecules: A Quantum Theory", Oxford University Press, Oxford (1990).

[52] Schmid N., Eichenberger A.P., Choutko A., Riniker S., Winger M., Mark A.E., Van Gunsteren W.F., Definition and Testing of the GROMOS Force-Field Versions 54A7 and 54B7, *Eur. Biophys. J.*, **40**: 843-856 (2011).

[53] Stroet M., Caron B., Visscher K.M., Geerke D.P., Malde A.K., Mark A.E., Automated Topology Builder Version 3.0: Prediction of Solvation Free Enthalpies in Water and Hexane, *J. Chem. Theory Comput.*, **14**: 5834-5845 (2018).

[54] Darden T., York D., Pedersen L., Particle Mesh Ewald: An N.log (N) Method for Ewald Sums in Large Systems, *J. Chem. Phys.*, **98**: 10089-10092 (1993).

[55] Hess B., Kutzner C., Van Der Spoel D., Lindahl E., GROMACS 4: Algorithms for Highly Efficient, Load-Balanced, and Scalable Molecular Simulation, *J. Chem. Theory Comput.*, **4**: 435-447 (2008).

[56] Parrinello M., Rahman A., Polymorphic Transitions in Single Crystals: A New Molecular Dynamics Method, *J. Appl. Phys.*, **52**: 7182-7190 (1981).

[57] Nosé S., A Molecular Dynamics Method for Simulations in the Canonical Ensemble, *Mol. Phys.*, **52**: 255-268 (1984).

[58] Verlet L., Computer "Experiments" on Classical Fluids. I. Thermodynamical Properties of Lennard-Jones Molecules, *Phys. Rev.*, **159**: 98 (1967).

[59] Delano W.L., PyMOL: An Open-Source Molecular Graphics Tool (2002).

[60] Khadim A.T., Albayati T.M., Cata Saady N.M., Desulfurization of Actual Diesel Fuel onto Modified Mesoporous Material Co/MCM-41, *Environ. Nanotechnol. Monit. Manag.*, **17**: 100635 (2022).